

Enhanced Emission and Its Switching in Fluorescent Organic Nanoparticles

Byeong-Kwan An,[†] Soon-Ki Kwon,[‡] Sang-Don Jung,[§] and Soo Young Park*

Contribution from the School of Materials Science & Engineering, Seoul National University, Seoul, 151-744, Korea, Department of Polymer Science & Engineering, Gyeongsang National University, Chinju, 660-701, Korea, and Basic Research Laboratory, Electronics & Telecommunications Research Institute, Daejeon, 305-350, Korea

Received May 15, 2002

Abstract: A new class of organic nanoparticles (CN-MBE nanoparticles) with a mean diameter of ca. 30–40 nm, which exhibit a strongly enhanced fluorescence emission, were prepared by a simple reprecipitation method. CN-MBE (1-cyano-*trans*-1,2-bis-(4'-methylbiphenyl)ethylene) is very weakly fluorescent in solution, but the intensity is increased by almost 700 times in the nanoparticles. Enhanced emission in CN-MBE nanoparticles is attributed to the synergetic effect of intramolecular planarization and J-type aggregate formation (restricted excimer formation) in nanoparticles. On/off fluorescence switching for organic vapor was demonstrated with CN-MBE nanoparticles.

Introduction

Fluorescent inorganic semiconductor or metal nanoparticles have attracted considerable research interests due to their unique properties originating from quantum-size effects.¹ They have been extensively investigated for various potential applications including the fluorescent biological labels,² photovoltaic cells,³ light-emitting diodes (LEDs),⁴ and optical sensors.⁵ As far as the application is concerned, fluorescent organic nanoparticles (FONs) are expected to hold the higher potentials because FONs allow much more variability and flexibility in materials synthesis and nanoparticle preparation. Investigations on the FONs, however, are only at their very initial stages presently. Systematic research works on FONs have been initiated by Nakanishi and co-workers,^{6–9} who have demonstrated that perylene and phthalocyanine nanoparticles show very different and size-

dependent fluorescent properties from those of bulk samples. Recently, Yao et al. reported similar results with pyrazoline nanoparticles.¹⁰

Motivated by the attractive potentials of FONs particularly for the nanosized optoelectronic devices applications, we have been engaged in the synthesis of a new class of strongly fluorescent organic molecules which spontaneously assemble into a stable FON. 1-Cyano-*trans*-1,2-bis-(4'-methylbiphenyl)ethylene (CN-MBE) is a typical molecule of our work which formed extremely uniform and stable FON with unusual fluorescence behavior. It was observed that the fluorescence emission from the CN-MBE nanoparticle is extremely strong, although CN-MBE itself is nonfluorescent in dilute solution. This fluorescence change is quite unusual considering that the fluorescence efficiency of organic chromophores generally decreases in the solid state, although they show high fluorescence efficiency in solution. This decreasing fluorescence efficiency in the solid state is quite general and is mainly attributed to the intermolecular vibronic interactions which induce the nonradiative deactivation process, that is, fluorescence quenching, such as excitonic coupling, excimer formations, and excitation energy migration to the impurity traps.¹¹ Very recently, however, several exceptional cases are being reported for a few organic fluorophores such as arylethynyl compounds,¹² poly(phenyleneethynylene)s,¹³ poly(phenylenevinylene) derivative,¹⁴ pentaphenylsilole,¹⁵ and pseudoisocyanine derivatives,¹⁶ which all together show unique enhanced emission rather than a fluorescence quenching in the solid state. Although the origins

* To whom correspondence should be addressed. E-mail: parksy@plaza.snu.ac.kr.

[†] Seoul National University.

[‡] Gyeongsang National University.

[§] Electronics & Telecommunications Research Institute.

- (1) (a) Brus, L. E. *J. Chem. Phys.* **1984**, *80*, 4403–4409. (b) Alivisatos, A. P. *Science* **1996**, *271*, 933–937. (c) Empedocles, S. A.; Bawendi, M. G. *Science* **1997**, *278*, 2114–2117.
- (2) (a) Bruchez, M.; Moronne, M.; Gin, P.; Weiss, S.; Alivisatos, A. P. *Science* **1998**, 2013–2016. (b) Michalet, X.; Pinaud, F.; Lacoste, T. D.; Dahan, M.; Bruchez, M. P.; Alivisatos, A. P.; Weiss, S. *Single Mol.* **2001**, *2*, 261–276.
- (3) Hagfeldt, A.; Grätzel, M. *Chem. Rev.* **1995**, *95*, 49–68.
- (4) Schlamp, M. C.; Peng, X.; Alivisatos, A. P. *J. Appl. Phys.* **1997**, *82*, 5837–5842.
- (5) (a) Wohltjen, H.; Snow, A. W. *Anal. Chem.* **1998**, *70*, 2856–2859. (b) Shipway, A. N.; Katz, E.; Willner, I. *ChemPhysChem* **2000**, *1*, 18–52.
- (6) Kasai, H.; Yoshikawa, Y.; Seko, T.; Okada, S.; Oikawa, H.; Matsuda, H.; Watanabe, A.; Ito, O.; Toyotama, H.; Nakanishi, H. *Mol. Cryst. Liq. Cryst.* **1997**, *294*, 173–176.
- (7) Kasai, H.; Kamatani, H.; Okada, S.; Oikawa, H.; Matsuda, H.; Nakanishi, H. *Jpn. J. Appl. Phys.* **1996**, *34*, L221–L223.
- (8) Kasai, H.; Kamatani, H.; Yoshikawa, Y.; Okada, S.; Oikawa, H.; Watanabe, A.; Ito, O.; Nakanishi, H. *Chem. Lett.* **1997**, 1181–1182.
- (9) Komai, Y.; Kasai, H.; Hirakoso, H.; Hakuta, Y.; Okada, S.; Oikawa, H.; Adschiri, T.; Inomata, H.; Arai, K.; Nakanishi, H. *Mol. Cryst. Liq. Cryst.* **1998**, *322*, 167–172.

(10) Fu, H.-B.; Yao, J.-N. *J. Am. Chem. Soc.* **2001**, *123*, 1434–1439.

(11) Birks, J. B. In *Photophysics of Aromatic Molecules*; Wiley: London, 1970.

(12) Levitus, M.; Schmieder, K.; Ricks, H.; Shimizu, K. D.; Bunz, U. H. F.; Garcia-Garibay, M. A. *J. Am. Chem. Soc.* **2001**, *123*, 4259–4265.

(13) Deans, R.; Kim, J.; Machacek, M. R.; Swager, T. M. *J. Am. Chem. Soc.* **2000**, *122*, 8565–8566.

(14) Belton, C.; O'Brien, D. F.; Blau, W. J.; Cadby, A. J.; Lane, P. A.; Bradley, D. D. C.; Byrne, H. J.; Stockmann, R.; Hörhold, H.-H. *Appl. Phys. Lett.* **2001**, *78*, 1059–1061.

of these enhanced emissions are still in debate, it is assumed that this unique fluorescence change is more or less related to the effects of intramolecular planarization or a specific aggregation (H- or J-aggregation) in the solid state. Enhanced fluorescence observed in CN-MBE FON seems to belong to this category of unusual fluorescence, while it is importantly noted as a unique observation in a nanoparticle medium.

In this paper, we report a synthesis and fluorescence behavior of CN-MBE nanoparticles with specific discussions on the possible origin of enhanced emission. Application of CN-MBE FON to the organic vapor sensor is also demonstrated in this work.

Results and Discussion

CN-MBE nanoparticles were prepared by a simple precipitation method without surfactants. By this method,¹⁷ water was used as a nonsolvent for CN-MBE in THF. After 60% volume fractions of water addition, CN-MBE (2×10^{-5} mol L⁻¹) in mixture solution started to aggregate into nanosize particles. Nanoparticles' suspensions were very transparent with no precipitates and were observed to be stable even after 3 months. This long-term stability was also observed for several surfactant-free organic nanoparticles in water.^{7,8,10} Recently, Abe et al. have shown that particular hydrophobic compounds which have polar C=O groups and high viscosity are stable in water for at least a year after nanoparticles' preparation without surfactants.¹⁸ This stability is ascribed to the formation of a particular structure around the polar groups which induces the negative ζ potential in nanoparticles. Electrostatic repulsion due to the negative ζ potential presumably prevents flocculation/coalescence of nanoparticles in water. We have found from experiment that CN-MBE nanoparticles which also possess polar cyano groups showed a negative ζ potential from -3 to -5 mV. Most probably, the excellent stability of CN-MBE nanoparticles seems to be related to this negative ζ potential. The shape of nanoparticles was observed by field emission scanning electron microscopy (FE-SEM). FE-SEM images in Figure 1 show that CN-MBE nanoparticles obtained by 80% volume fractions of water addition are very fine spheres with a mean diameter of about 30–40 nm.

CN-MBE showed a dramatic change of fluorescence intensity from the nonfluorescent isolated single molecule in THF to the strongly fluorescent nanoparticles' suspension in THF/water mixtures (Figure 2a). This enhanced emission from CN-MBE nanoparticles is clearly depicted by the changes of relative quantum yield (Φ_f) of CN-MBE (2×10^{-5} mol L⁻¹) in various fractions of THF/water mixtures (Figure 2b).¹⁹ Isolated CN-MBE up to 50% volume fractions of water addition shows

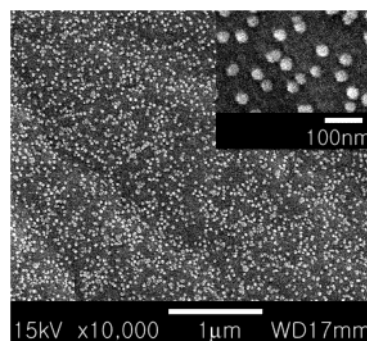


Figure 1. SEM images of CN-MBE nanoparticles obtained from nanoparticles' suspension containing 80% volume fractions of water in THF. Inset shows the magnified SEM image.

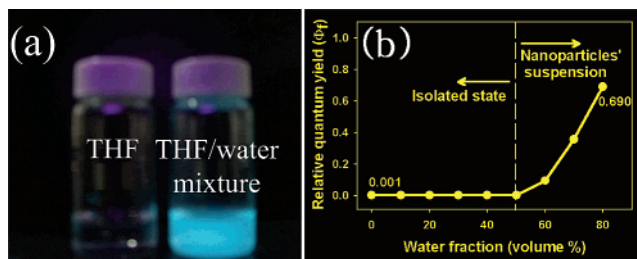


Figure 2. (a) The fluorescence emission of CN-MBE (2×10^{-5} mol L⁻¹) in THF (left) and THF/water mixture (80% volume fractions of water) (nanoparticles' suspension) (right) under the UV light (365 nm). (b) Relative quantum yields (Φ_f) of CN-MBE (2×10^{-5} mol L⁻¹) depending on water fractions in THF.

virtually no fluorescence at all ($\Phi_f = 0.001$), whereas the Φ_f values increase drastically from 60% volume fractions of water addition when CN-MBE starts to form nanoparticles. In the case of 80% volume fractions of water addition, the Φ_f value of CN-MBE nanoparticles' suspension is almost 700 times higher than that of CN-MBE solution in THF.

In recent years, a few cases of enhanced emission in the solid state of specific organic molecules have been reported and interpreted in terms of the intra- and intermolecular effects exerted by fluorophore aggregation.^{12–16,20,21} Intramolecular effects on fluorescence enhancement are simply explained by the conformational changes of chromophores. It is supposed that the twisted conformations of chromophores in solution tend to suppress the radiative process, whereas planar ones of chromophores induced in the solid state activate the radiation process.^{22–24} Intermolecular effects by aggregation also influence the fluorescence changes in π -conjugated organic chromophores. Effects on fluorescence changes by intermolecular interactions are correlated with the aggregation morphology such as H-type or J-type aggregation. H-aggregates where molecules are aligned parallel to each other with strong intermolecular interaction tend to induce the nonradiative deactivation process.¹¹ Formation of H-aggregates is characterized by blue-shifted absorption bands with respect to those of the isolated chromophore.²⁵ In contrast,

(15) (a) Luo, J.; Xie, Z.; Lam, J. W. Y.; Cheng, L.; Chen, H.; Qiu, C.; Kwok, H. S.; Zhan, X.; Liu, Y.; Zhu, D.; Tang, B. Z. *Chem. Commun.* **2001**, 1740–1741. (b) Luo, J.; Xie, Z.; Lam, J. W. Y.; Cheng, L.; Chen, H.; Qiu, C.; Kwok, H. S.; Zhan, X.; Liu, Y.; Zhu, D.; Tang, B. Z. *Chem. Eng. News* **2001**, 79 (41), 29.

(16) (a) Jelly, E. E. *Nature* **1936**, 138, 1009–1010. (b) Scheibe, G. *Angew. Chem.* **1936**, 49, 563.

(17) For general preparation methods of organic nanoparticles, see: (a) Kasai, H.; Nalwa, H. S.; Okada, S.; Oikawa, H.; Nakanish, H. *Handbook of Nanostructured Materials and Nanotechnology*; Academic Press: New York, 2000; Vol. 5, Chapter 8, 433–473. (b) Horn, D.; Rieger, J. *Angew. Chem., Int. Ed.* **2001**, 40, 4330–4361.

(18) Kamogawa, K.; Akatsuka, H.; Matsumoto, M.; Yokoyama, S.; Sakai, T.; Sakai, H.; Abe, M. *Colloids Surf., A* **2001**, 180, 41–53.

(19) Fluorescence quantum yields (Φ_f) were calculated using 9,10-diphenylanthracene (DPA) in benzene as a standard reference: Berlman, I. B. *Handbook of Fluorescence Spectra of Aromatic Molecules*; Academic Press: New York, 1971.

(20) Walters, K. A.; Ley, K. D.; Schanze, K. S. *Langmuir* **1999**, 15, 5676–5680.

(21) Miteva, T.; Palmer, L.; Kloppenburg, L.; Neher, D.; Bunz, U. H. F. *Macromolecules* **2000**, 33, 652–654.

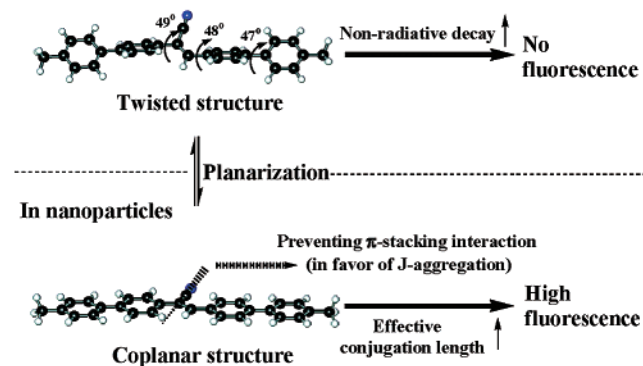
(22) Oelkrug, D.; Tompert, A.; Egelhaaf, H.; Hanack, M.; Steinhuber, E.; Hohloch, M.; Meier, H.; Stalmach, U. *Synth. Met.* **1996**, 83, 231–237.

(23) Oelkrug, D.; Tompert, A.; Gierschner, J.; Egelhaaf, H.; Hanack, M.; Hohloch, M.; Steinhuber, E. *J. Phys. Chem. B* **1998**, 102, 1902–1907.

(24) Souza, M. M.; Rumbles, G.; Gould, I. R.; Amer, H.; Samuel, I. D. W.; Moratti, S. C.; Holmes, A. B. *Synth. Met.* **2000**, 111–112, 539–543.

(25) Gruszecki, W. I. *J. Biol. Phys.* **1991**, 18, 99–109.

Scheme 1. Proposed Mechanism of Enhanced Emission in CN-MBE Nanoparticles
In dilute solution



J-aggregates where the molecules are arranged in head-to-tail direction induce a relatively high fluorescence efficiency with a bathochromic shift of UV absorption maximum.²⁵

The enhanced fluorescence emission in CN-MBE nanoparticles (Figure 2) is also explained in terms of the intra- and intermolecular effects. CN-MBE consists of two biphenyl molecules with a cyano-stilbene moiety as a bridging group. The optimized geometry of CN-MBE in the gas phase was calculated by using the PM3 parametrization in the HyperChem 5.0 program (Hypercube). It was obtained that isolated CN-MBE molecules are twisted by the steric interactions in biphenyl unit²⁶ as well as the bulky cyano group attached into vinylene moiety²⁷ (Scheme 1). It is well known that the conformation of the neighboring phenyl rings in biphenyl molecules is determined by the opposing influences of the intramolecular repulsion of *ortho*-hydrogen atoms and intermolecular packing forces.²⁸ Conformational studies on biphenyl and PPP oligomers have revealed that a more planar conformation is favored in a crystalline environment, even though the twist conformation is preferred in the isolated state.^{28,29} The observed planarity in the crystalline state is mainly due to the fact that constraints within the unit cell might be strong enough to overcome the *ortho*-hydrogen repulsions.^{28,29} Similar conformational changes also have been observed in the case of the *trans*-stilbene unit in poly(*p*-phenylene vinylene) (PPV) oligomers³⁰ and twisted aryl-ethynyl compounds.¹²

Therefore, the CN-MBE molecule consisting of the biphenyl and substituted stilbene unit is likely to show similar conformational planarization due to the aggregation in a nanoparticle.

Unlike the almost perfect planarization of biphenyl and stilbene compound in a crystal,^{29,30} CN-MBE is speculated to be somewhat twisted even after aggregation because there are additional steric interactions caused by the cyano group in CN-MBE. As a result of this conformation change, however, the fluorescent property of CN-MBE seems to be altered as to induce the enhanced fluorescence emission.

It is considered that the aggregation-induced planarization extends the effective conjugation length and increases the oscillator strength of CN-MBE. Semiempirical AM1 calculations supported this postulation. The UV absorption maximum (λ_{\max}) and magnitude of oscillator strength (f) at λ_{\max} increase from the twisted form ($\lambda_{\max} = 341$ nm, $f = 1.41$) to the planar form ($\lambda_{\max} = 379$ nm, $f = 1.53$) of CN-MBE. Therefore, aggregation-induced planarization is considered as one of the probable mechanisms of enhanced emission for CN-MBE nanoparticles.

It is also expected that the aggregation-induced planarization inevitably causes unique intermolecular interactions in nanoparticles. It is well known that the strong intermolecular interactions are aroused in the solid state of planar π -conjugated chromophores which induce the formation of excimer complex leading to the fluorescence quenching.¹¹ The bulky and polar cyano group in CN-MBE, however, plays an important role of restricting the parallel face-to-face intermolecular interactions in the aggregated state.^{22,23} Preventing parallel orientation of conjugated chromophores tends to favor J-aggregation with enhanced fluorescence emission instead of H-aggregation in the solid state. The J-aggregation mechanism for the enhanced fluorescence was already observed in the pseudoisocyanine (PIC) dye which was characterized by the twisted structure and bulky groups preventing face-to-face intermolecular interaction.^{31,32}

Therefore, most probably, the enhanced emission of CN-MBE is attributed to the combined effects of aggregation-induced planarization and J-aggregate formation. This postulated mechanism of enhanced emission in CN-MBE nanoparticles is depicted in Scheme 1.

Our speculation on the mechanism of enhanced emission is supported by the experimental UV and photoluminescence (PL) data of CN-MBE nanoparticles. From 60% volume fractions of water addition, when the nanoparticles begin to form, the maximum peaks in the absorption spectra of CN-MBE are red-shifted, and a new shoulder band appears around 420 nm (Figure 3a). The inset of Figure 3a shows the resolved absorption bands located at 366 and 420 nm, respectively. The 366 nm band is associated with the π - π^* transition of the CN-MBE molecule which is red-shifted from that in dilute solution (342 nm). This bathochromic effect indicates that effective conjugation length of CN-MBE is extended from the isolated twisted molecule to the planar one in nanoparticles. This result is also in accord with the calculated absorption band shift from the twisted conformer to the planar conformer (Figure 3a, bottom). On the

(26) The dihedral torsional angle of 44.4° in biphenyl molecules has been widely recognized as the reference value for theoretical calculations: Allmendinger, A.; Bastiansen, O.; Fernholt, L.; Cyvin, B. N.; Cyvin, S. J.; Samdal, S. *J. Mol. Struct.* **1985**, *128*, 59–76.

(27) It is well known that cyano groups attached into vinylene linkage with phenyl rings cause the deformation of coplanarity, see refs 22–24 and Lange, F.; Hohnholz, D.; Leuze, M.; Ryu, H.; Hohloch, M.; Freudenmann, R.; Hanack, M. *Synth. Met.* **1999**, *101*, 652–653.

(28) (a) Baker, K. N.; Fratini, A. V.; Resch, T.; Knachel, H. C.; Adams, W. W.; Soccia, E. P.; Farmer, B. L. *Polymer* **1993**, *34*, 1571–1587. (b) Corish, J.; Morton-Blake, D. A.; O'Donoghue, F.; Baudour, J. L.; Bénére, F.; Toudic, B. *J. Mol. Struct.* **1995**, *358*, 29–38. (c) Guha, S.; Graupner, W.; Resel, R.; Chandrasekhar, M.; Chandrasekhar, H. R.; Glaser, R.; Leising, G. *Phys. Rev. Lett.* **1999**, *82*, 3625–3628.

(29) In the gaseous and solution state, biphenyl molecules show a twisted conformation between two phenyl rings, with a dihedral angle estimated from electron diffraction as 42–45°. At room temperature, however, the biphenyl molecule in the crystal is practically planar. (a) Trotter, J. *Acta Crystallogr.* **1961**, *14*, 1135–1140. (b) Hargreaves, A.; Rizvi, S. H. *Acta Crystallogr.* **1962**, *15*, 365–373. (c) Ambrosch-Draxl, C.; Majewski, J. A.; Vogl, P.; Leising, G. *Phys. Rev. B* **1995**, *51*, 9668–9676. (d) Brédas, J. L.; Thémans, B.; Fripiat, J. G.; André, J. M.; Chance, R. R. *Phys. Rev. B* **1984**, *29*, 6761–6773.

(30) The ab initio calculation and electron diffraction analysis suggested that *trans*-stilbene is not planar (ca. 20–30°) in the isolated state, whereas the structure was proved to be nearly planar (ca. 3.4–6.8°) in the crystalline state by X-ray diffraction analysis. (a) Woo, H. S.; Lhost, O.; Graham, S. C.; Bradley, D. D. C.; Friend, R. H.; Quattrocchi, C.; Brédas, J. L.; Schenk, R.; Müllen, K. *Synth. Met.* **1993**, *59*, 13–28. (b) Traetteberg, M.; Frantsen, E. B.; Mijlhoff, F. C.; Hoekstra, A. J. *Mol. Struct.* **1975**, *26*, 57–68. (c) Tian, B.; Zerbi, G.; Müllen, K. *J. Chem. Phys.* **1991**, *95*, 3198–3207. (d) Lagowski, J. B. *J. Mol. Struct.* **2002**, *589–590*, 125–137.

(31) Yoshika, H.; Nakatsu, K. *Chem. Phys. Lett.* **1971**, *11*, 255–258.

(32) Bujdák, J.; Iyi, N.; Hrobáriková, J.; Fujita, T. *J. Colloid Interface Sci.* **2002**, *247*, 494–503.

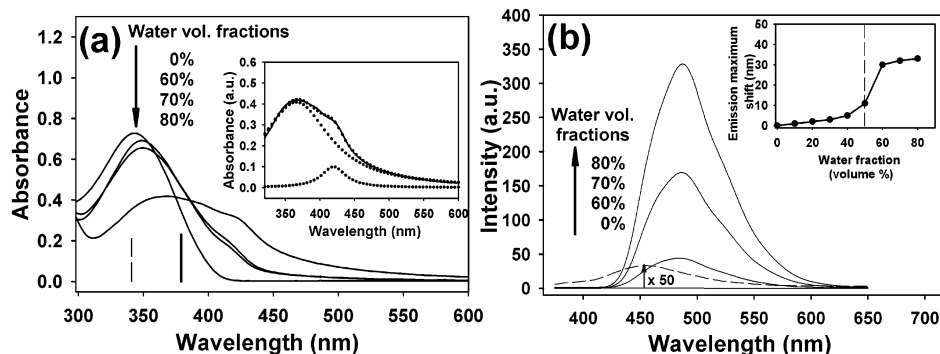


Figure 3. (a) UV absorption spectra changes of CN-MBE (2×10^{-5} mol L $^{-1}$) depending on the water fractions in THF. The calculated absorption maximum peaks of twisted (dot line) and planar form (solid line) of CN-MBE are shown at the bottom. Inset shows peak separation of CN-MBE nanoparticles in the case of 80% water addition. (b) PL spectra changes of CN-MBE (2×10^{-5} mol L $^{-1}$) depending on the water fractions in THF. Inset shows the change in the emission maximum peak of CN-MBE.

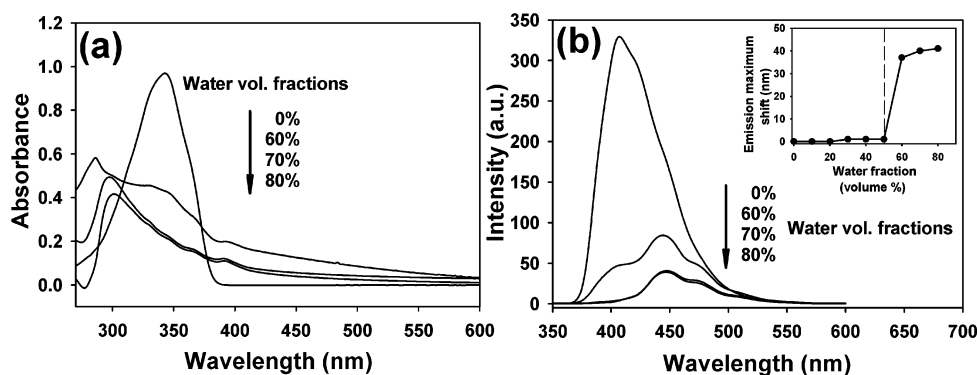


Figure 4. (a) UV absorption spectra changes of DPST (2×10^{-5} mol L $^{-1}$) depending on the water fractions in THF. (b) PL spectra changes of DPST (2×10^{-5} mol L $^{-1}$) depending on the water fractions in THF. Inset shows the changes in the emission maximum peak of DPST.

other hand, the band at 420 nm is assigned to the J-aggregates of CN-MBE. In general, the J-aggregation band is distinctly red-shifted and appears as an intense narrow absorption band due to the motional narrowing,³³ but that of CN-MBE nanoparticles in Figure 3a is relatively broad and weak. This result suggests that the molecules in nanoparticles may be oriented in a less optimal way of J-aggregation. Lattice disorder is considered as one of the possible reasons of it.³⁴

Extended conjugation and J-aggregation lead to the dramatic increase of the fluorescence intensity in CN-MBE nanoparticles as shown in Figure 3b. It is seen that the fluorescence intensity of CN-MBE increases discontinuously from 60% volume fractions of water addition as shown in Figure 3b. The inset of Figure 3b shows that the peak position of fluorescence emission is also red-shifted discontinuously above 60% volume fractions of water.

It is supposed that the cyano group in CN-MBE is effective in reducing the face-to-face intermolecular interaction in nanoparticles which consequently induces the formation of J-aggregates as was observed in pseudoisocyanine (PIC) molecules. To investigate the role of the cyano group, the UV and PL spectra of CN-MBE were compared with those of a reference model compound, *trans*-4,4'-diphenylstilbene (DPST), which lacks only the cyano group from CN-MBE. Both CN-MBE and DPST show high energy tails in the visible region of the UV

absorption spectrum above 60% volume fractions of water additions when nanoparticles are formed (Figures 3a and 4a, respectively). These tails in the visible region are attributed to Mie scattering caused by nanosized particles.³⁵ The striking difference of UV absorption spectra between CN-MBE and DPST is the direction of spectral shift. As nanoparticles are formed, absorption maximum peaks of CN-MBE are red-shifted, while those of DPST are blue-shifted. The blue shift is explained by H-aggregate formation resulting from the strong π -stacking interactions, which is consistent with many other spectroscopic findings.^{35,36} In contrast to the drastic increase of CN-MBE emission, the emission intensity of DPST showed a drastic decrease in nanoparticles (Figures 3b and 4b, respectively). New red-shifted bands at around 450 and 480 nm of DPST are attributed to the excimer formation by H-aggregation.

Application of CN-MBE nanoparticles to the on/off fluorescence switches was investigated by use of the different fluorescence intensity in solution and nanoparticles. Under the 365 nm of UV light illumination at room temperature, CN-MBE nanoparticles on the TLC plate show bright blue fluorescence which switches off reversibly in the atmosphere of dichloromethane vapor (Figure 5). This fluorescence switching behavior of CN-MBE nanoparticles provides a novel concept of nanosized fluorescence switches which sense organic vapors.

(33) (a) Rossi, U. D.; Daehne, S.; Reisfeld, R. *Chem. Phys. Lett.* **1996**, *251*, 259–267. (b) Tachibana, H.; Sato, F.; Terrettaz, S.; Azumi, R.; Nakamura, T.; Sakai, H.; Abe, M.; Matsumoto, M. *Thin Solid Films* **1998**, *327–329*, 813–815. (c) Ilharco, L. M.; Brito de Barros, R. *Langmuir* **2000**, *16*, 9331–9337. (d) Eisfeld, A.; Briggs, J. S. *Chem. Phys.* **2002**, *281*, 61–70.

(34) Knapp, E. W. *Chem. Phys.* **1984**, *85*, 73–82.

(35) Auweter, H.; Haberkorn, H.; Heckmann, W.; Horn, D.; Lüddecke, E.; Rieger, J.; Weiss, H. *Angew. Chem., Int. Ed.* **1999**, *38*, 2188–2191.

(36) (a) Kasha, M.; Rawls, H. R.; El-Bayoumi. *Pure Appl. Chem.* **1965**, *11*, 371–393. (b) Ruban, A. V.; Horton, P.; Young, A. J. *J. Photochem. Photobiol., B* **1993**, *21*, 229–234. (c) Dähne, L.; Biller, E. *Adv. Mater.* **1998**, *10*, 241–245.

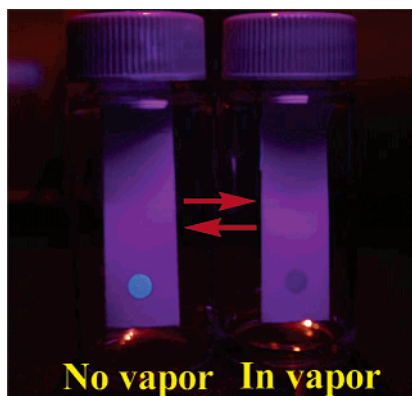


Figure 5. On/off fluorescence switching of MBAN nanoparticles on the TLC plate without vapor (left) and in vapor (dichloromethane) (right) under UV light (365 nm) illumination at room temperature.

In conclusion, we have demonstrated a new class of fluorescent organic nanoparticles (CN-MBE FONs) which are very fine spheres with a mean diameter of about 30–40 nm. They exhibit a strongly enhanced emission and on/off fluorescent switching which senses organic vapor. Enhanced fluorescence emission in CN-MBE nanoparticles was attributed to the synergetic effect of planarization and J-aggregation (restricted excimer formation).

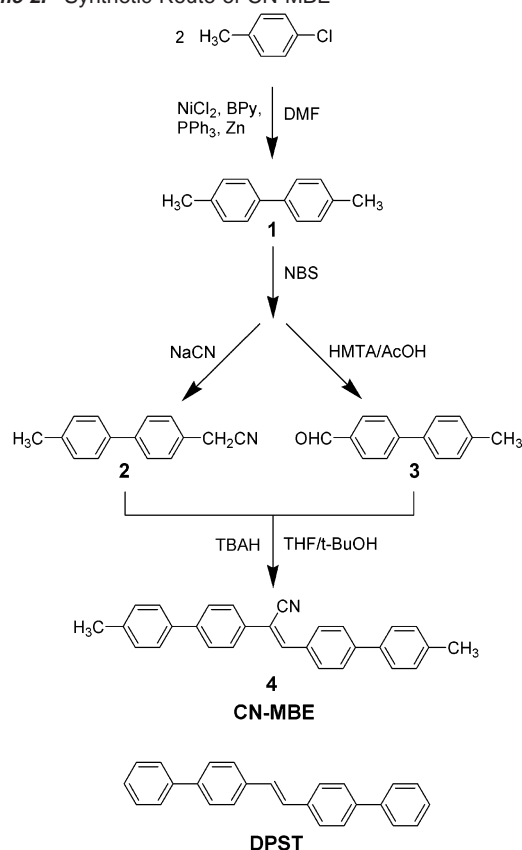
Experimental Section

Synthesis. 4,4'-Dimethyl Biphenyl (1). 4-Chlorotoluene (79 mmol) was added to the mixture of nickel chloride (3.9 mmol), 2,2'-bipyridine (BPy) (3.9 mmol), triphenylphosphine (PPh₃) (15.7 mmol), and zinc (122.3 mmol) in *N,N*-dimethylformamide (DMF) solution (50 mL). The mixture was stirred at 90 °C for 5 h. After being cooled, 1 N HCl solution was poured into the reaction mixture. The precipitate was filtered and washed with methanol (yield: 75%). ¹H NMR (300 MHz, CDCl₃) δ [ppm]: 7.49 (d, 4H, Ar-H), 7.25 (d, 4H, Ar-H), 2.38 (s, 6H, -CH₃). MS (EI) (calcd for C₁₄H₁₄, 182.26; found, 182) *m/e*: 182, 167, 152, 128, 115, 90, 76, 63, 51.

(4'-Methylbiphenyl-4-yl)acetonitrile (2). *N*-Bromosuccinimide (NBS) (13.3 mmol) was added to a solution of **1** (13.3 mmol) in benzene (40 mL), and the mixture was refluxed for 12 h. The mixture was poured into a 500 mL of water and stirred for 2 h. After the solvent was removed under vacuum, the residue was added into a solution of NaCN (51.2 mmol) in tetrahydrofuran (THF) (30 mL). The mixture was stirred at 50 °C for 24 h. After being cooled to room temperature, the resulting mixture was column chromatographed on silica gel, eluting with ethyl acetate/hexane (1:3 by volume) solvent. After solvent was removed under vacuum, the solid product was obtained (45%). ¹H NMR (300 MHz, CDCl₃) δ [ppm]: 7.58 (d, 2H, Ar-H), 7.47 (d, 2H, Ar-H), 7.40 (d, 2H, Ar-H), 7.27 (d, 2H, Ar-H), 3.79 (s, 2H, -CH₂CN), 2.40 (s, 3H, -CH₃). MS (EI) (calcd for C₁₅H₁₃N, 207.27; found, 207) *m/e*: 207, 192, 165, 152, 139, 115, 89, 76, 63, 51.

4'-Methylbiphenyl-4-carboxaldehyde (3). Bromination reaction of **1** (13.3 mmol) was carried out by the same procedure as above. After bromination, the residue was added into a solution of hexamethylenetetramine (HMTA) (51.2 mmol) in chloroform (30 mL). The mixture was refluxed for 12 h. After being cooled to room temperature, the solvent was removed under vacuum. Next 50 mL of a glacial acetic acid (AcOH) and water mixture (1:1 by volume) was poured into the reaction mixture and refluxed for 2 h. The resulting mixture was column chromatographed on silica gel, eluting with ethyl acetate/hexane (1:3 by volume) solvent. After solvent was removed under vacuum, the solid product was obtained (25%). ¹H NMR (300 MHz, CDCl₃) δ [ppm]: 10.0 (s, 1H, -CHO), 7.95 (d, 2H, Ar-H), 7.75 (d, 2H, Ar-H), 7.55

Scheme 2. Synthetic Route of CN-MBE



(d, 2H, Ar-H), 7.28 (d, 2H, Ar-H), 2.42 (s, 3H, -CH₃). MS (EI) (calcd for C₁₄H₁₂O, 196.24; found, 196) *m/e*: 196, 165, 152, 115, 97, 82, 63, 51.

1-Cyano-*trans*-1,2-bis-(4'-methylbiphenyl)ethylene (CN-MBE) (4). The mixture of **2** (1 mmol) and **3** (1 mmol) in *tert*-butyl alcohol (7 mL) and THF (3 mL) was stirred at 50 °C for 1 h. Tetrabutylammonium hydroxide (TBAH) (1 M solution in methanol) (0.1 mL) was slowly dropped into the mixture and stirred for 1 h. The green precipitate was collected by filtration and washed with methanol (94%) (Scheme 2). ¹H NMR (300 MHz, CDCl₃) δ [ppm]: 7.98 (d, 2H, Ar-H), 7.69 (m, 6H, Ar-H), 7.58 (s, 1H, vinyl), 7.52 (d, 4H, Ar-H), 7.25 (d, 4H, Ar-H), 2.39 (s, 6H, -CH₃). FT-IR (KBr, cm⁻¹): 3040, 2950, 2220 (-CN attached to vinylene), 1500, 1150, 800. MS (EI) (calcd for C₂₉H₂₃N, 385.5; found, 385) *m/e*: 385, 370, 294, 278, 252, 193, 165, 105, 91, 65, 57. Anal. Calcd for C₂₉H₂₃N: C, 90.35; H, 6.01; N, 3.63. Found: C, 90.27; H, 5.94; N, 3.62.

***trans*-4,4'-Diphenylstilbene (DPST).** DPST (Lancaster, 99%) was purchased commercially and used as obtained without further purification.

Nanoparticles' Preparation. Distilled water was regularly injected into the chromophore/THF with vigorous stirring at room temperature, using a syringe pump. Before distilled water injection, distilled water and chromophore solution were filtered by membrane filter with 0.2 μm pore size. As volume fractions of injected distilled water increased, those of THF solution gradually decreased. In all samples, the concentration of chromophores (2 × 10⁻⁵ mol L⁻¹) was constant after distilled water injection.

Instrumentation. ¹H NMR spectra were recorded on a JEOL JNM-LA300 (300 MHz) in CDCl₃ solutions with CHCl₃ at 7.26 ppm as the internal standard. IR spectra were measured on a Midac FT-IR spectrophotometer using KBr pellets. Mass spectra were measured on a JMS AX505WA by EI mode. UV-visible absorption and fluorescence emission spectra were recorded on a HP 8452-A and a Shimadzu RF-500 spectrofluorophotometer, respectively. FE-SEM images were

acquired on a JSM-6330F (JEOL) by dropping nanoparticles' suspension on carbon tapes. The fluorescence displays of CN-MBE nanoparticles' suspension and CN-MBE nanoparticles on the TLC plate were photographed on a Nikon-Coolpix 995 digital camera. CN-MBE nanoparticles on the TLC plate were prepared by dropping nanoparticles' suspension using the same method for acquiring FE-SEM images of CN-MBE nanoparticles on the carbon tapes. The ζ potential of CN-MBE nanoparticles was measured by an electrophoretic light-scattering

spectrophotometer (ELS-8000) (Otsuka Electronics, Japan) using the standard sample of polystyrene latex particles.

Acknowledgment. This work was partly supported by ETRI, and we are grateful for the instrumental support from the equipment facility of CRM-KOSEF, Korea University. Helpful discussion with Prof. B. Z. Tang is greatly appreciated.

JA0269082